macQsimal	Title **Fibre-coupled THz imager setup**	Deliverable Number **D7.3**
Project Number **820393**		Version **1**

H2020-FETFLAG-2018-2021

macQsimal

Miniature **A**tomic vapor-**C**ell **Q**uantum devices for **S**ens**I**ng and **M**etrology **A**pp**L**ications

Deliverable 7.3

Fibre-coupled THz imager setup

WP7 – Atomic GHz & THz sensors and vector imagers

Authors: Shuying Chen (UDUR), Kevin Weatherill (UDUR)

Lead participant: UDUR

Delivery date: 30 September 2020

Dissemination level: Public

Type: R (Document, Report)

This work has received funding from the European Union's Horizon 2020 research and innovation programme under grant agreement No. 820393.

Revision History

Author Name (Partner short name)	**Description**	**Date**
Shuying Chen (UDUR) Kevin Weatherill (UDUR)	Draft deliverable	11.08.2020
Shuying Chen (UDUR) Kevin Weatherill (UDUR)	Revision 1	09.09.2020
Shuying Chen (UDUR) Lucy Downes (UDUR) Kevin Weatherill (UDUR)	Revision 2	29.09.2020
Philipp Treutlein (UNIBAS)	Review	30.09.2020
Shuying Chen (UDUR)	Final version	30.09.2020

Abbreviations

AMC	Amplifier multiplier chain
Cs	Caesium
fW	Femto Watt
Hz	Hertz
IR	Infrared
K	Potassium
kHz	Kilohertz
Li	Lithium
µW	Microwatt
Na	Sodium
PTFE	Polytetrafluoroethylene
Rb	Rubidium
S&K	SCHÄFTER + KIRCHHOFF GmbH
THz	Terahertz
WP	Work Package

Project partner short names

UDUR	University of Durham, UK
UNIBAS	Universität Basel, CH

Contents

Executive Summary

This deliverable is a report demonstrating our work towards the realisation of a compact THz imaging system. In the report, we introduce the field of THz imaging systems, noting key existing technologies and how these compare to our proposed Rydberg-based imaging system. We then show our achievement towards the goal of a fibre-coupled THz imaging system—making use of a line generator, we make the working distance of the laser set-up more compact.

Need for the Deliverable

This Deliverable 7.3 is required to address a more compact and portable THz imaging setup for future convenient applications -- a fibre-coupled device for THz imaging.

Objectives of the Deliverable

The deliverable intends to introduce a fibre-coupled compact THz imaging setup we have built for the future wider and more convenient industrial applications.

Outcomes

Using thermal Rydberg atoms, we have successfully built a prototype device of THz imaging with an achievable frame rate of over 3000 Hz, and the spatial resolution of less than 1mm, corresponding to the diffraction limit. The minimum detectable intensity is measured to be around 0.1 mW/m^2 at 550 GHz. To make the whole system more compact, we have made use of the commercial fibre-coupled telescope as the light line generator. As a result, we shorten the working distance of the system from 1000 mm for each beam into approximated 200 mm, making the system much more compact.

Next steps

The next steps include:

1) Demonstrate THz imaging using the new compact setup, e.g. to do various materials tests.
2) Try larger imaging areas by increasing the light sheet size in the cell.
3) Expand the technology to use Rubidium atomic vapour in the imaging system with fibre-coupled line generators.
4) Develop cheaper and more convenient home-made light line generators.
5) Try the micro vapour cells fabricated by CESM, which will potentially make the system even more compact.

1 Introduction

Terahertz waves form a part of the electromagnetic spectrum in frequency range from 100 GHz to 10 THz. It falls between microwave and infrared, the so-called 'THz gap' as shown in Figure 1. This frequency range is remarkable as it can penetrate various materials often associated with wrapping, such as plastic, fabric, paper, and card, but without damaging organic tissues as an x-ray would. This quality means that THz fields could prove useful for security tests, for example in airports or train stations [1], as well as in quality checking and defect detection [2, 3]. There is also interest in THz technology from the fields of biological and medical research for blood disease [4, 5] and oral cancer detection [6, 7]. So, THz imaging has wide potential applications in various fields [8].

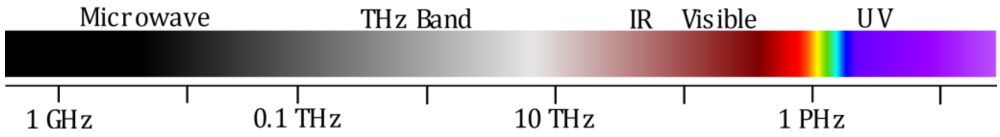

Figure 1. THz band gap.

However, THz imaging methods are in relative infancy as compared to microwave detection, with well-developed semiconductor technologies, or IR light detection with modern optical techniques. Currently, the principle methods of THz imaging include frequency up-conversion with nonlinear optical material such as diamond [9] or DAST crystal [10], transferring the THz field into optical photons; or single pixel capture method with Golay cells and bolometers or self-mixing in quantum cascade lasers (QCLs) [11]; or Focal Plane Arrays (FPAs), typically consisting of arrays of small point detectors such as micro bolometers [12, 13], field-effect transistors (FETs) [14] or carbon nanotubes [15], or even superconductors [16]. These methods have different advantages, but the common drawback though, is that their THz imaging frame rate is severely limited, which restrains the practical applications of THz imaging.

At UDUR we have realized an ultra-fast THz imaging system with demonstrated frame rates over 3 kHz [17]. These frame rates are much faster than the traditional methods, e.g. thermodynamic THz detectors [12, 13] and may pave the way to the wider practical applications of THz imaging. The system uses a thermal alkali atomic vapour as an efficient THz to optical transducer. In our detection system, the difficult to detect THz frequency is transferred into easy to detect visible fluorescence. The fluorescence can be detected easily with normal cheap optical cameras. The benefit of using highly excited "Rydberg" atoms is that they have larger dipole moments to response to THz field thus have higher sensitivity. In addition, the alkali atoms, including Li, Na, K, Rb, Cs, has hundreds of Rydberg levels which can be coupled to different THz frequencies, as shown in the Figure 2. The vapour alkali cell is also easy to fabricate with low cost for K, Rb and Cs atoms. Thus, our system provides a novel easy and cheap THz imaging method with ultrafast speed.

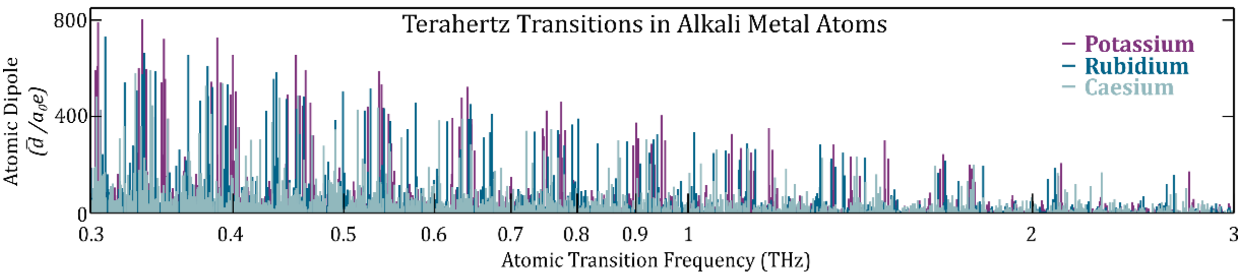

Figure 2. Useful transitions in K, Rb, Cs atoms for the different THz frequency couplings. Y axis is the atomic dipole moment, and x axis is possible THz transition frequencies.

To make the whole THz imaging system more convenient to apply in various situation, we need to make the optical-table-top experiment much more compact. One reasonable proposal is to make use of optical fibre coupling to generate light sheet to shorten the working distance. Here we report that we realized a more compact system by using a fibre-coupled line generator.

2 Rydberg Imaging System Outline

We make use of the thermal Cs Rydberg atomic ensemble to realize the THz field imaging. The principle is that we utilize a three-step IR laser excitation to prepare the Cs atoms to a Rydberg state. And the Rydberg Cs atoms then couple the THz field. When the THz field is turned on, the Cs Rydberg atoms are coupled to another specific Rydberg state. The states' energy difference is just the THz field energy. The atoms in that THz Rydberg state then decay to lower energy levels and finally to the ground states. Without the THz coupling, the atoms in the original Rydberg states will decay via several paths to the ground states, thus radiate different wavelength photons, showing visible orange fluorescence from the mixture of wavelengths from the different decaying paths. However, when the THz is on, the atoms are in another Rydberg state, and a particular decay path is strongly enhanced. The atomic cell radiates bright green fluorescence. People can use normal optical cameras to capture the fluorescence from the cell to give the image information of the THz field.

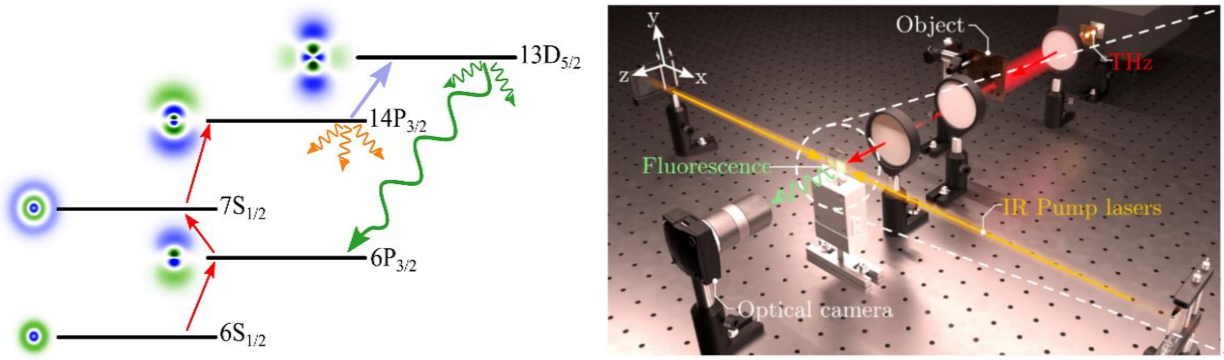

Figure 3. Cs atomic energy levels used (left) and the THz imaging experimental setup (right) [17].

The energy levels of Cs atoms used are shown as the left figure in Figure 3 [17]. The three excitation steps are as below. The Cs atoms from ground state of $6\mathrm{S}_{1/2}$ are excited to $6\mathrm{P}_{3/2}$ with a first laser of wavelength 852 nm, and then from $6\mathrm{P}_{3/2}$ excited to $7\mathrm{S}_{1/2}$ with a second laser of wavelength 1470 nm, and finally $7\mathrm{S}_{1/2}$ is excited to high excited Rydberg state $14\mathrm{P}_{3/2}$ with the third laser 843 nm. After the atoms are prepared in the high Rydberg state, a THz field of frequency 0.55 THz is used to resonantly couple the levels $14\mathrm{P}_{3/2}$ to another Rydberg level $13\mathrm{D}_{5/2}$, resulting in the emission of strong green fluorescence from the decay path from $13\mathrm{D}_{5/2}$ to $6\mathrm{P}_{3/2}$. The centre wavelength of the fluorescence is 535 nm, which is captured by the optical camera.

The schematic of the imaging system experimental setup is shown in the right panel of Figure 3 [17]. The Cs vapour is contained within a cuboid quartz cell and heated to 50 Celsius degrees with a resistive metal-ceramic heater. The outer size of the cell is 10 mm × 10 mm × 50 mm. The atoms are prepared using co-axial IR laser beams shaped such that a 100 µm thick sheet of excited atoms is formed in the xy plane. The third laser 843 nm counter-propagates with the first and second lasers to reduce the Doppler Effect. The three lasers run continuously, and the first two lasers are frequency-stabilized with the sub-Doppler polarization spectroscopy [18]. The continuous-wave THz field (up to 19 µW at 0.55 THz) is emitted from a microwave-seeded amplifier multiplier chain (AMC) and propagates in the z direction, perpendicular to the plane of the vapour. And then the THz field are imaged on that atomic area after going through the object and a PTFE aspherical lenses imaging system (as in Figure 3). The fluorescence emitted by atoms when the THz is on is re-imaged onto an optical camera, providing an image of the incident THz field with the information of the object shape. Narrow band optical filters are used to increase the signal to noise ratio.

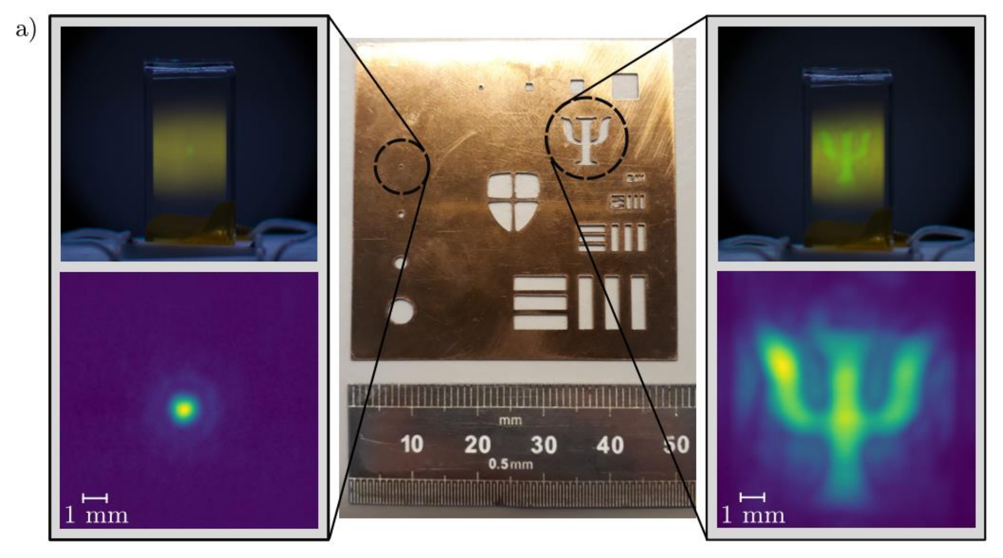

Figure 4. A real image of 'Ψ' in the cell from the metal mask [17]. A metal mask (centre) placed in the object plane of the system. Top left and right are true-colour images taken for a 0.50-mm-diameter pinhole (left) and a "Ψ"-shaped aperture (right). Down left and right are the images with narrow band filters in the system for 535 nm wavelength to increase the signal to noise ratio.

Figure 4 shows an example of the THz imaging of a 'Ψ' sign in the cell from a metal mask in the THz beam path. The spatial resolution achieved here is 1 mm, reaching the diffraction limit of the system. The minimum detectable power is 190 fW per pixel [17].

The most advantageous part of this system is for the high-speed imaging capability. Fig. 5 is an example of fast speed video recorded for water dropping after being released from a burette with the image frame rate of 500 Hz. The THz imaging speed can be as fast as 3000 Hz frame rate [17].

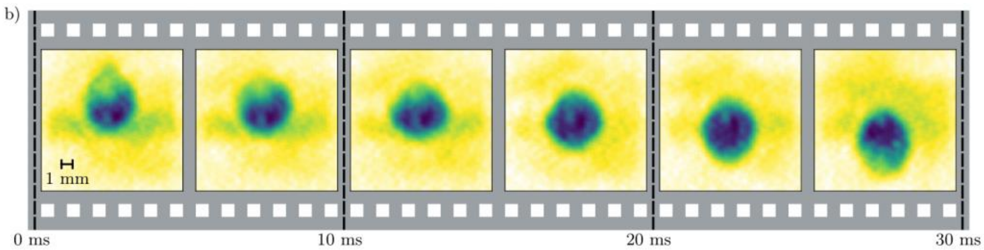

Figure 5. Ultrahigh-speed THz video of water droplet [17].

In conclusion, we realized the thermal Rydberg atomic THz imaging system with high imaging frame rate as well as high resolution in the lab. To make it more convenient in industry applications, we need to make the system more compact. Thus, in the next section, we introduce the fibre-coupled telescope for generating the light sheet in the cell to make the system more compact.

3 Fibre-coupled Telescope

To make the whole imaging system more compact for more convenient applications in industrial applications, we proposed the idea to make use of the fibre-coupled telescope in the system to generate the expanded light. Because of our need to have an extended illumination area of ~ $1cm^2$ we need to create a light sheet with a Rayleigh range of ~1cm. This means that it is impossible to directly fibre-couple a laser to the vapour cell, as we need a significant optical path length to expand the excitation beam. The compromise solution we have achieved is to use a customized fibre-coupled line generator from SCHÄFTER + KIRCHHOFF GmbH (S&K). It is a one-piece telescope made of 11 elements. The device details are shown as below in subsection 3.1 and the beam profile performance we tested for the light sheet is demonstrated in subsection 3.2.

3.1 Setup overview

The fibre-coupled line generator is purchased from S&K company for our third step laser 843nm. Because of the commercial copyright, the design details are not fully provided. The known parameters and models of the components for the line generator are listed as below:

Table 1. Parameter table.

Parameter Table	(11 elements in 8 groups) Aligned for 852 nm *Assuming an effective fibre NA 0.078 (1/e^2)
Fibre collimator:	type 60FC-E-4-F18x72-852
Effective focal length:	18.2x72 mm / NA 0.15
Beam elliptical	1:4
Focussing optics:	cylindrical f' 200 mm
Line* approx.:	10 mm x 70 µm (1/e^2)
Rayleigh range approx.:	2zR = 11 mm
Working distance approx.:	190 mm
Housing:	Ø 32/34.5 mm
AR:	750 - 980 nm / clear aperture: Ø 21.5 mm
Inclined coupling axis:	FC-APC connection

The key features are seen that the working distance of the device is 190 mm and it can produce a light sheet with the size of 10 mm × 70 µm (1/e^2). Rayleigh range is 11 mm which is good enough for our 10 mm long cuboid cell.

The experimental setup scheme with the S&K line generator is shown as below in Figure 6, compared to the original setup before using the line generator where we used traditional cylindrical lenses and mirrors is as in Figure 7. In Figure 6, two reflected mirrors after the line generator are used to help with the alignment to overlap with the other two beams. The real working distance for the third step laser

(843 nm) is 190 mm. While compared to the initial working distance in Figure 7 which is around 1000 mm from the fibre collimator to the cell, the optical path with the line generator is as 20% short as before.

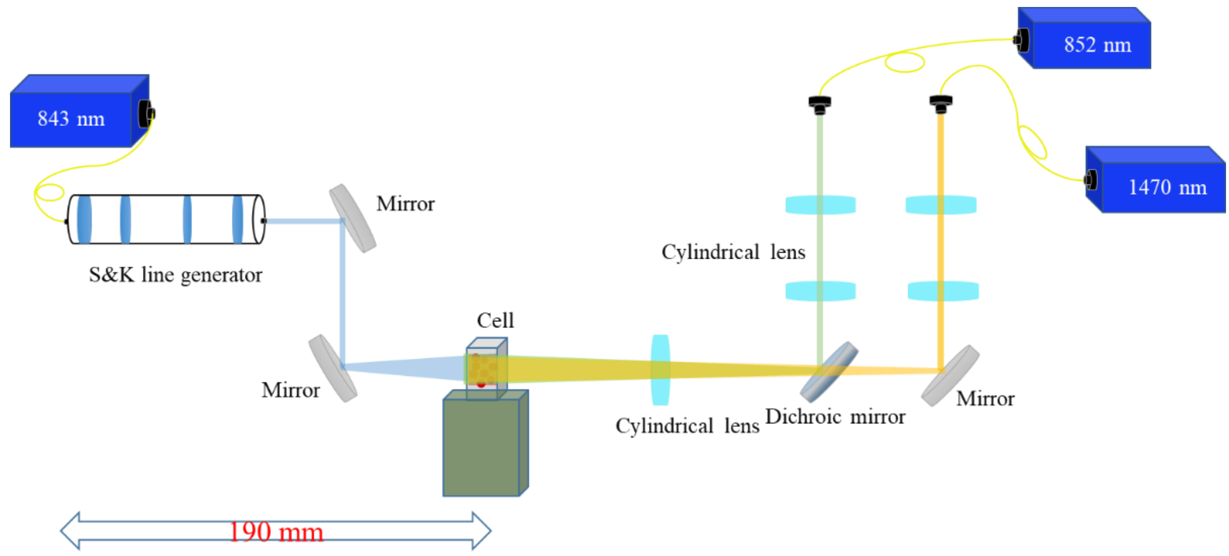

Figure 6. Optical line generation setup with S&K company product. THz source and camera are not included here. The working distance of the S&K line generator for 843 nm laser is 190 mm. The line generator shown here is just a schematic diagram.

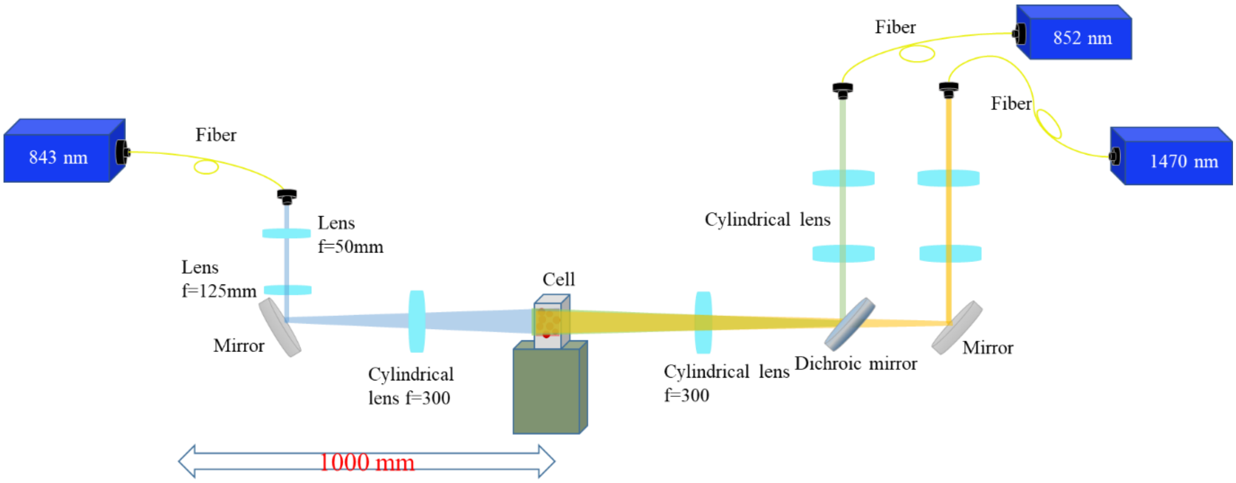

Figure 7. Optical line generation setup for imaging with cylindrical lenses. THz source and camera are not included here. The total working distance of 843 nm laser from fibre collimator through mirrors to the cell is 1000 mm.

3.2 Beam profile test

Next, we test the beam profile performance for 843 nm output from the S&K line generator. Here we make use of the knife-edge method [19] to measure the beam profile, because the vertical size of the light sheet is 10 mm, which is too large for the normal beam profiler or camera.

With the knife-edge method, the beam profile data for 843 nm laser is shown as below in Figure 8. The measured beam waist is ~60 µm (1/e^2) in the horizontal direction, so the total diameter of the light sheet in the horizontal direction is 120 µm. That satisfies our requirements for the imaging experiment that the beam waist is less than half the terahertz wavelength (full terahertz wavelength we use is 550 µm).

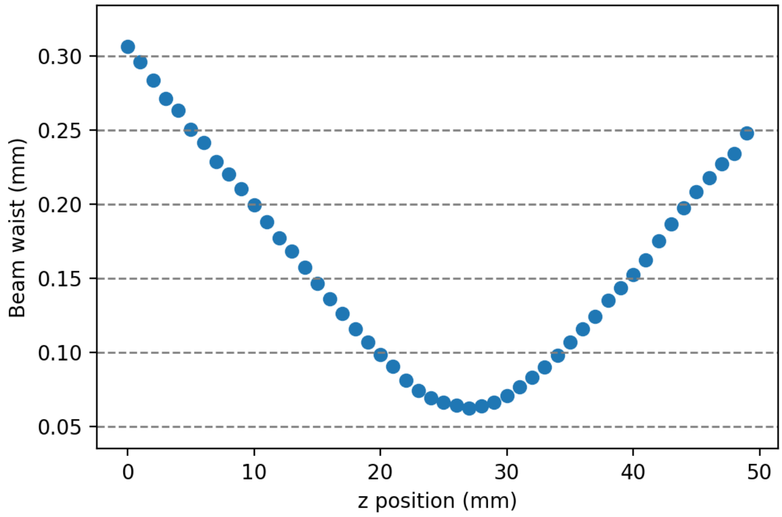

Figure 8. Beam profile of 843 nm laser. The round dots are experimental data and the beam waist of 843 nm is shown as 60 µm (1/e^2).

To check the adaptability of the line generator for the first step laser (852 nm), we also test the line generator with 852 nm laser input. The data is as below in Figure 9. The beam waist size for 852 nm laser from the line generator is ~50 µm, slightly smaller than for 843 nm, which also satisfies the requirement for our imaging experiment.

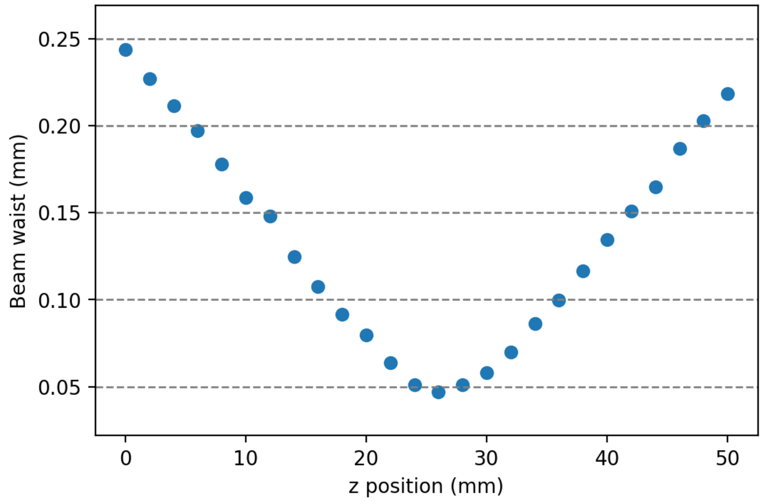

Figure 9. Beam profile for the first step laser 852nm. The round dots are experimental data and the beam waist of 852 nm is ~50 µm (1/e^2).

In conclusion, the S&K line generator is useful to realize a relatively compact imaging setup, resulting a new working distance that is only 20% of the original optical path length. And the line generator works for both the first step laser of 852 nm and the third step laser 843 nm. The second beam (at 1470 nm) is outside the transmission window of the AR-coating of the line generator, so we still, for now, use free space cylindrical lenses and mirrors to produce the light sheet.

4 Future plan

After successfully realizing the thermal Rydberg atomic THz imaging system, we made the imaging system 80% shorter by using S&K line generator. Thus, it is very promising to make a portable THz imaging system with following explorations as the future plan:

1. Take more images for THz with the new fibre-coupled compact setup.
2. Develop multiple sizes of light sheet for larger image area for THz imaging.
3. Continue setting up a Rb system for THz imaging with the fibre-coupled line generators, which will be sensitive to more THz frequencies.
4. Develop home-made line-generator, which can be cheaper and more flexible.
5. Test the micro vapour cells fabricated by CESM. With the microcells, we can couple the lasers through the same window of the cell, and it is possible to make the system become more compact.

References

[1] Kemp, Michael C., et al. "Security applications of terahertz technology." *Terahertz for Military and Security Applications*. Vol. 5070. International Society for Optics and Photonics, 2003.

[2] Ellrich, Frank, et al. "Terahertz quality inspection for automotive and aviation industries." *Journal of Infrared, Millimeter, and Terahertz Waves,* 41.4 (2020): 470-489.

[3] Ahi, Kiarash, and Mehdi Anwar. "Advanced terahertz techniques for quality control and counterfeit detection." *Terahertz Physics, Devices, and Systems X: Advanced Applications in Industry and Defense*. Vol. 9856. International Society for Optics and Photonics, 2016.

[4] Danciu, Mihai, et al. "Terahertz spectroscopy and imaging: a cutting-edge method for diagnosing digestive cancers." *Materials* 12.9 (2019): 1519.

[5] Wan, Min, John J. Healy, and John T. Sheridan. "Terahertz phase imaging and biomedical applications." *Optics & Laser Technology* 122 (2020): 105859.

[6] Pawar, Ashish Y., et al. "Terahertz technology and its applications." *Drug invention today* 5.2 (2013): 157-163.

[7] Sim, Yookyeong Carolyn, et al. "Terahertz imaging of excised oral cancer at frozen temperature." *Biomedical optics express* 4.8 (2013): 1413-1421.

[8] Mittleman, Daniel M. "Perspective: Terahertz science and technology." *Journal of Applied Physics* 122.23 (2017): 230901.

[9] Clerici, Matteo, et al. "CCD-based imaging and 3D space–time mapping of terahertz fields via Kerr frequency conversion." *Optics letters* 38.11 (2013): 1899-1901.

[10] Fan, Shuzhen, et al. "Diffraction-limited real-time terahertz imaging by optical frequency up-conversion in a DAST crystal." *Optics Express* 23.6 (2015): 7611-7618.

[11] Dean, Paul, et al. "Absorption-sensitive diffuse reflection imaging of concealed powders using a terahertz quantum cascade laser." *Optics Express* 16.9 (2008): 5997-6007.

[12] Lee, Alan WeiMin, and Qing Hu. "Real-time, continuous-wave terahertz imaging by use of a microbolometer focal-plane array." *Optics letters* 30.19 (2005): 2563-2565.

[13] Lee, Alan WM, et al. "Real-time imaging using a 4.3-THz quantum cascade laser and a 320/spl times/240 microbolometer focal-plane array." *IEEE Photonics Technology Letters* 18.13 (2006): 1415-1417.

[14] Qin, Hua, et al. "Room-temperature, low-impedance and high-sensitivity terahertz direct detector based on bilayer graphene field-effect transistor." *Carbon* 116 (2017): 760-765.

[15] Suzuki, D., S. Oda, and Y. Kawano. "A flexible and wearable terahertz scanner." *Nature Photonics* 10.12 (2016): 809-813.

[16] Ariyoshi, Seiichiro, et al. "Superconducting detector array for terahertz imaging applications." *Japanese journal of applied physics* 45.10L (2006): L1004.

[17] Downes, Lucy A., et al. "Full-Field Terahertz Imaging at Kilohertz Frame Rates Using Atomic Vapor." *Physical Review X* 10.1 (2020): 011027.

[18] Khosrofian, John M., and Bruce A. Garetz. "Measurement of a Gaussian laser beam diameter through the direct inversion of knife-edge data." *Applied optics* 22.21 (1983): 3406-3410.

[19] Carr, Christopher, Charles S. Adams, and Kevin J. Weatherill. "Polarization spectroscopy of an excited state transition." *Optics Letters* 37.1 (2012): 118-120.